Global and Planetary Change 73 (2010) 114–122

Contents lists available at ScienceDirect

Global and Planetary Change

journal homepage: www.elsevier.com/locate/gloplacha

An Early–Middle Guadalupian (Permian) isotopic record from a mid-oceanic carbonate buildup: Akiyoshi Limestone, Japan

Masaaki Musashi [a,*], Yukio Isozaki [a], Hodaka Kawahata [b]

[a] Department of Earth Science and Astronomy, The University of Tokyo, Komaba, Meguro, Tokyo 153-8902, Japan
[b] Graduate School of Frontier Sciences, The University of Tokyo, Kashiwa 277-8561, Japan

ARTICLE INFO

Article history:
Accepted 26 March 2010
Available online 8 June 2010

Keywords:
Guadalupian
carbon isotope
Panthalassa
high productivity
Kamura event
Akiyoshi
paleo-atoll

ABSTRACT

In order to understand the oceanographic changes before the Guadalupian–Lopingian (Permian) boundary mass extinction event, we investigated the isotopic compositions of the inorganic carbon and the oxygen ($\delta^{13}C_{carb}$ and $\delta^{18}O_{carb}$) of the Guadalupian (Middle Permian) shallow marine carbonates deposited on a seamount-top in the superocean Panthalassa. The drilled samples were obtained at Kaerimizu in the Akiyoshi area, SW Japan. We focused on the Roadian-Wordian (Middle Guadalupian) interval that spans over 7 fusuline zones; i.e. the *Parafusulina kaerimizuensis* Zone (*Pk* Z.), *Afghanella ozawai* Zone (*Ao* Z.), *Neoschwagerina craticulifera robusta* Zone (*Ncr* Z.), *Verbeekina verbeeki–Afghanella schenki* Zone (*Vv–As* Z.), *Neoschwageina fusiformis* Zone (*Nf* Z.), *Verbeekina verbeeki* Zone (*Vv* Z.), and *Colania douvillei* Zone (*Cd* Z.), in ascending order. Analytical results showed that the $\delta^{13}C_{carb}$ values stayed almost constant around +3.0‰ PDB in the *Pk* Z., *Ao* Z. and the lower half of the *Ncr* Z., and those in the upper-section gradually decreased down to −2.0‰, of which the lowest was found in the *Cd* Z.
We statistically extracted the samples with presumably better preserved $\delta^{13}C_{carb}$ values in the Kaerimizu section ranged between +0.5 and +4.0‰ with average values of $\delta^{13}C_{carb}$ of +2.7 ± 1.0‰, on the basis of $\delta^{13}C_{carb}$–$\delta^{18}O_{carb}$ characterization. This interval shows a monotonous decrease in $\delta^{13}C_{carb}$ values from ca +4.0‰ to +2.0‰. This indicates that the primary productivity might be generally high in the Wordian mid-oceanic domain but slightly declined in the Late Wordian. The studied Early-Middle Guadalupian interval is chemostratigraphically correlated with the other mid-Pansalassan paleo-atoll limestone e.g. Iwato Formation in Japan, suggesting that the relatively high $\delta^{13}C_{carb}$ (over +3.0‰) of seawater predominated in shallow mid-superocean during the middle Middle Permian.

1. Introduction

The catastrophic mass extinction at the end of Permian is the one of the largest events in the history of the Earth's life, although the cause of the event is still in discussion. Recent studies confirm that the extinction has occurred in two steps: the first at the Guadalupian–Lopingian boundary (G–LB) and the second at the Permian–Triassic boundary (P–TB) (e.g., Stanly and Yang, 1994; Jin et al., 1994; Isozaki, and Ota, 2001). The apparent coincidence in timing between the first extinction and the onset of the P–TB superanoxia in the superocean Panthalassa (Isozaki, 1997a) suggests that a global-scale environmental change has started around the G–LB to modify the pre-existing long-lasting stable conditions during the Early–Middle Permian.

Stable carbon isotope ratio ($\delta^{13}C$ vs. PDB, ‰) is a commonly used geochemical proxy to monitor global environmental changes in the past, as preliminarily performed for the P–TB event (e.g., Baud et al., 1989; Heydari et al., 2003; Korte et al., 2005). The latest studies focused on the G–LB event clarified a sharp negative shift of the $\delta^{13}C$ values across the boundary at GSSP (Global Stratotype Section and Point) of the G–LB in South China (Wang et al., 2004).

The previous studies investigated mostly on the Permo-Triassic shallow marine shelf sequences deposited around the supercontinent Pangea, but not much on mid-oceanic rocks deposited in Pansalassa simply because the concurrent oceanic rocks were already subducted thus are difficult to obtain from the modern oceanic domain. Nonetheless, in order to elucidate the cause of the extinction event, information on the environmental conditions of the Guadalupian oceans immediately before the G–LB appears to be essential. Musashi et al. (2001, 2007) first overcame this problem of biased information source by studying P–TB mid-oceanic shallow marine carbonates contained in the Jurassic accretionary complexes in Japan. As to the Middle Permian interval, Isozaki et al. (2007a,b) lately documented a secular change in seawater $\delta^{13}C$ value also across the G–LB in mid-oceanic paleo-atoll limestone, and further clarified a unique interval with high positive $\delta^{13}C$ values (over +5‰) within the Capitanian, Upper Guadalupian. They named this remarkable positive isotopic excursion the Kamura event, and speculated that the appearance of a cool interval during the Late Guadalupian was probably related to the G–LB extinction. Isozaki et al. (2007b) emphasized that the volatile

* Corresponding author. Present address: Department of Chemistry, Tokyo Metropolitan University, 1-1 Minamiosawa, Hachioji, Tokyo 192-0397 Japan. Tel./fax: +81 42 4677 1111.
E-mail address: mmusashi@tmu.ac.jp (M. Musashi).

0921-8181/$ – see front matter © 2010 Elsevier B.V. All rights reserved.
doi:10.1016/j.gloplacha.2010.03.013

fluctuation in C isotope ratio of seawater had started in the Capitanian, although the pre-Capitanian secular change in mid-Panthalassa has not yet been fully clarified.

In order to check the Early–Middle Guadalupian carbon isotope trend in seawater of open ocean before the Kamura event, this study analyzed the secular change of C isotope in the Roadian–Wordian (Lower–Middle Guadalupian) carbonates in Akiyoshi, SW Japan (Fig. 1), that were derived from an oceanic seamount complex in the westernmost Panthalassa. Here, we present the analytical results on carbon and oxygen isotope compositions of the bulk carbonates from the Guadalupian part of the Carboniferous to Permian Akiyoshi Limestone, and discuss their geochemical significance.

2. Geological setting

The Akiyoshi belt in SW Japan is underlain mainly by the Upper Permian accretionary complex that includes numerous exotic blocks of Upper Paleozoic deep-sea chert and basaltic greenstones and also clastics-free shallow marine carbonates of paleo-seamount origin (Kanmera et al., 1990; Sano and Kanmera, 1988). The Middle Carboniferous to Middle Permian Akiyoshi Group, nearly 700 m-thick, occurred as fragmented exotic blocks surrounded by the latest Permian mudstone matrices (Fig. 1b). This shallow marine reef-type limestone deposited primarily as an atoll complex on the top of a hotspot-type seamount in the middle of the superocean Panthalassa (e.g., Kanmera and Nishi, 1983; Sano and Kanmera, 1988), and later accreted to Japan (South China) margin by oceanic subduction (Fig. 1c; Isozaki, 1997b).

The Akiyoshi Limestone Group has long been known as a classic section for high-resolution fusuline zonation of the Late Carboniferous to Middle Permian in East Asia. In particular, the Kaerimizu section in the northern Akiyoshi area (Fig. 1) exposes more than 10 fusuline zones of the Early to Middle Permian in sequence, as demonstrated by intense surface mapping and drilled core research (Ota et al., 1973; Ueno, 1992, 1996; Nakazawa and Ueno, 2004). Judging from the narrow age gap between the carbonate sedimentation and the tectonic accretion, the Akiyoshi paleo-seamount was

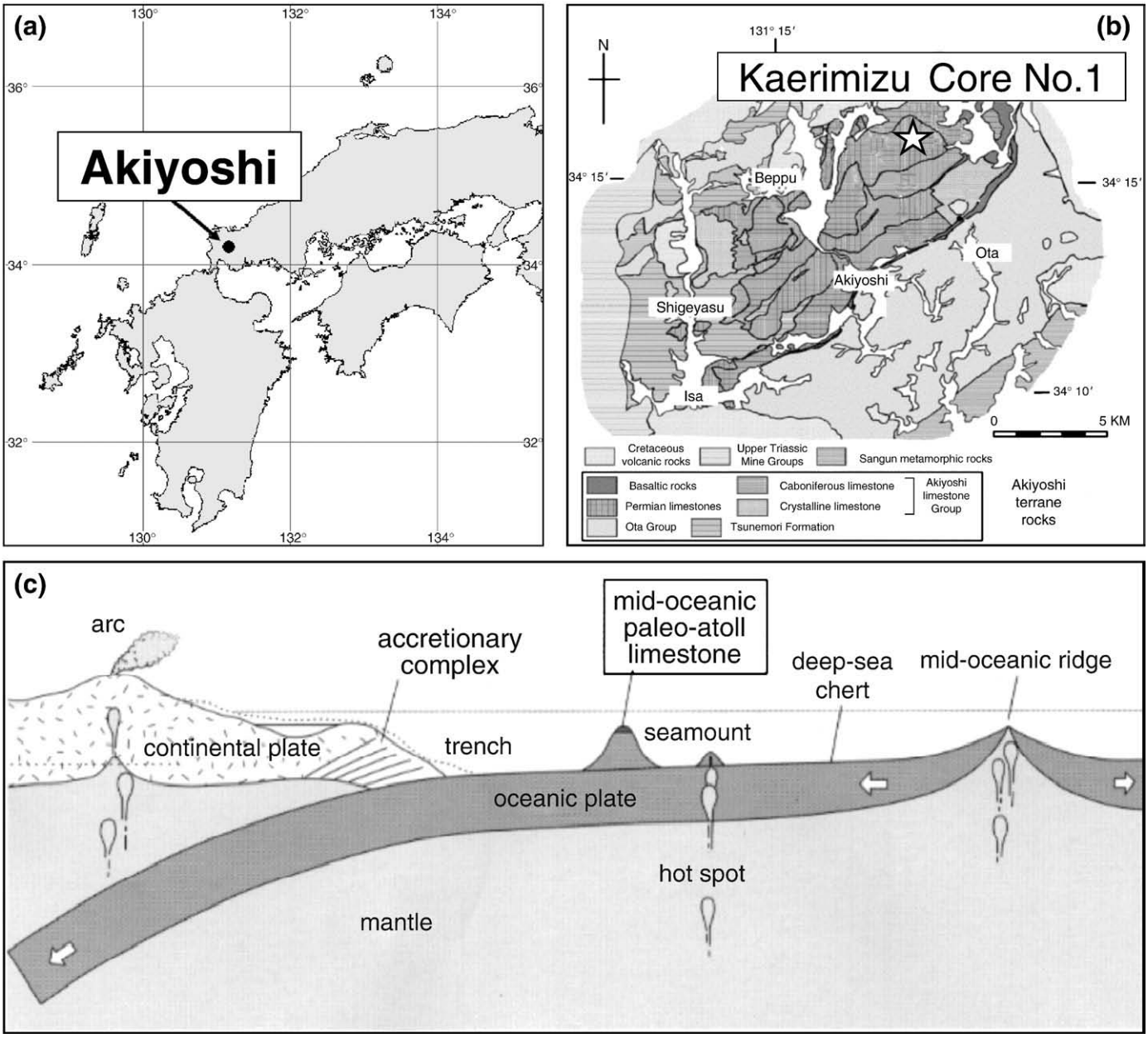

Fig. 1. Index map of (a) the Akiyoshi area in Japan and (b) the Kaerimizu drilling site. The geological map was modified from Kanmera and Nishi (1983) and Sano (2006). (c) The Akiyoshi Limestone was originated from the shallow marine reef-type limestone accreted to Japan (South China) margin by oceanic subduction (Isozaki, 1997b).

located off SW Japan (= eastern South China) active margin, probably within some hundreds of kilometers from the trench, during the Middle Permian (Maruyama et al., 1997).

In order to analyze environmental change during the Guadalupian, we focused on the upper part of the Akiyoshi Limestone Group, particularly on the upper Roadian to Wordian (Early–Middle Guadalupian) interval at Kaerizmizu. This interval composed entirely of shallow marine bioclastic limestone was recovered almost completely by drilling at the "Kaerimizu doline (a term for a local depression in Karst topography)" (Ota et al., 1973). We employed samples of the Kaermizu core no.1 drilled at the Kaerimizu doline for this study by the courtesy of the Akiyoshi-dai Museum of Natural History. We analyzed a ca. 162 m-thick interval of the drilled core that was composed of the *Neoschwagerina simplex* Zone (*Ns* Z.), the *Parafusulina kaerimizuensis* Zone (*Pk* Z.), *Afghanella ozawai* Zone (*Ao* Z,), *Neoschwagerina craticulifera robusta* Zone (*Ncr* Z.), *Verbeekina verbeeki–Afghanella schenki* Zone (*Vv–As* Z.), *Neoschwagerina fusiformis* Zone (*Nf* Z.), *Verbeekina verbeeki* Zone (*Vv* Z.), and *Colania douvullei* Zone (*Cd* Z.) in stratigraphically ascending order (Fig. 2). The fusuline zones used in this study is after Ota et al. (1973) and Nakazawa and Ueno (2004), with a slight modification through our own microscopic studies helped by H. Igo who identified fusulines from the core samples. The *Ns* Z. is correlated with the Roadian at its

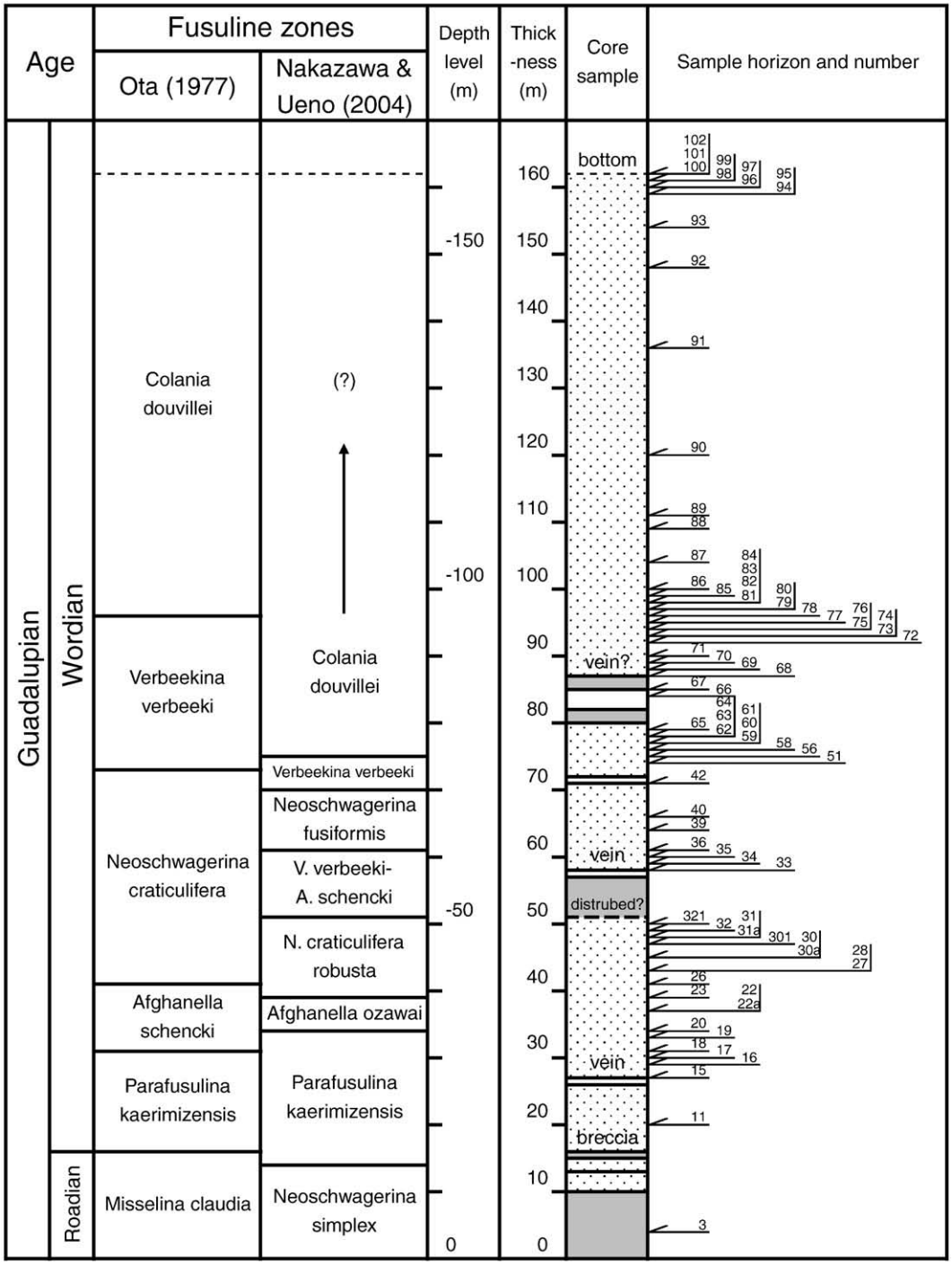

Fig. 2. Stratigraphic column of the Akiyoshi–Kaerimizu core no.1 section. The sample positions in the core were indicated with their number (see Table 1). For comparison, fusuline biozones by Ota (1977) and Nakazawa and Ueno (2004) were shown. Lithological description of the core samples is after Nakazawa and Ueno (2004): the dark gray part indicates lime-mudstone dominated facies, and the dotted part the grain- and pack-stone dominated facies, respectively.

stratotype in Texas, whereas all other zones with the Wordian. No Capitanian fusulines were found at the Kaerimizu doline. Thus in short, the studied section ranges in the Roadian to Wordian, and the uppermost part of the Wordian interval is probably missing. As the Permian limestone is structurally overturned around Kaerimizu, the oldest part of the section (*Pk* Z.) apparently occurs at the top of the drilled core, whereas the youngest (*Cd* Z,) at the bottom. The first appearance horizons of the fusuline assemblages, the *Pk* Z., *Ao* Z., *Ncr* Z., *Nf* Z., and *Cd* Z. reported by Nakazawa and Ueno (2004), were confirmed in our study at 14, 34, 39, 61, and 74 m-level of the core, respectively.

The apparent thickness of the *Cd* Z. in the Kaerimizu core is obviously larger than that examined at the surface outcrop (Ueno, 1992). This disagreement in thickness suggests that the *Cd* Z. may have been structurally repeated at least twice (the interval from AK1-91 to 102 may represent the same interval from AK1-86 to 90) probably through underground blind faulting related to subduction–accretion tectonics. There are some horizons with disturbed features; i.e., a thin brecciated zone at 50.4 m (at the top of the *Ncr* Z.), and zones with concentrated calcite veins at 56.7 and 73 m-levels (at the bottom of the *Vv–As* Z. and that in middle of the *Vv* Z.).

The stratigraphic column of the studied core with sample horizons from Kaerimizu is shown in Fig. 2. For 75 fresh limestone samples from 5 to 162 m-level of the core, stable carbon and oxygen isotope ratios of bulk carbonates were measured. They include one sample (AK1-3) from the *Ns* Z., 7 samples (AK1-11 to 20) from the *Pk* Z., 3 samples (AK1-22 to 23) from the *Ao* Z., 11 samples (AK1-26 to 321) from the *Ncr* Z., 2 samples (AK1-33 and 34) from the *Vv-As* Z., 4 samples (AK1-35 to 40) form the *Nf* Z., 2 samples (AK1-42 and 51) from the *Vv* Z., and 45 samples (AK1-58 to 102) from the *Cd* Z.

3. Experimental

The samples were collected from the vein-free part of the core chips, crushed into pieces, transferred to a beaker filled with Milli-Q-ultra pure water, and were agitated for a few minutes in an ultrasonic bath. After being dried in air at room temperature, the sample pieces were powered and stored in a sample container. The $\delta^{13}C_{carb}$ values of the most of samples were analyzed at Geological Survey of Japan, the Advanced Institute of Science and Technology (AIST) in Japan and twelve samples (AK1-75 to AK1-86) were at the University of Utrecht (UU) in the Netherlands. Several samples were analyzed at both laboratories for cross-checking.

Carbon and oxygen isotope compositions of the 75 samples ($\delta^{13}C_{carb}$ and $\delta^{18}O_{carb}$) were analyzed by the isotope ratio mass-spectrometers: VG SIRA 24 EM of the UU and Micromass Optima mass spectrometer at the AIST, Japan. Precisions of the stable isotopic value were greater than 0.1‰ (1 σ) for both $\delta^{13}C$ and $\delta^{18}O$ at the AIST (Suzuki et al., 2000). We checked the correlation of the $\delta^{13}C$ and $\delta^{18}O$ values between two laboratories, which shows a fairly good agreement. Therefore, it requires no calibration between the stable isotopic values at both laboratories, as long as the Pee Dee Belemnite (PDB) standard are regularly applied for the data calibration.

Hereafter, all of the $\delta^{13}C_{carb}$ and $\delta^{18}O_{carb}$ values analyzed at AIST together with those values at UU for the samples (AK1-75 and -86) were chosen for this discussion.

4. Results

The analytical results on the inorganic carbon and oxygen isotope compositions of the bulk carbonate ($\delta^{13}C_{carb}$ and $\delta^{18}O_{carb}$ vs. PDB) of the samples were shown in Table 1. Fig. 3ab shows that $\delta^{13}C_{carb}$ and $\delta^{18}O_{carb}$ secular changes in interval between 4.7 and 162.63 m-levels of the core section.

The $\delta^{13}C_{carb}$ values of all samples ranged between −2.1‰ (AK1-90) and +4.3‰ (AK1-15) with the average value of +1.3‰. They steadily decreased from +4.1‰ of 30 m-level in *Pk* Z. to −1.5‰ of 120 m-level in *Cd* Z. In the *Ncr* Z., the values became lighter with approaching to the boundary between *Ncr* Z. and *Vv–As* Z. The $\delta^{18}O_{carb}$ values ranged between −15.0‰ (AK1-88) and −5.5‰ (AK1-39), and became specifically depleted in the bottom and top of the studied section. The $\delta^{13}C_{carb}$ was +3.2‰ at 4.1 m-level, and slightly increased to +4.2‰ at 37.40 m-level, and then gradually deceased down to +1.2‰ between 37.40 and 73.50 m-level with the *Ncr* Z. Then, the $\delta^{13}C_{carb}$ increased again to +2.9‰ from 73.50 to 77.30 m-level, and decreased to −1.5‰ at 85.56 m-level of the core. The $\delta^{13}C_{carb}$ slightly increased to 0.8‰, however, it soon decreased, and stayed at around −0.5‰ afterward.

The $\delta^{18}O_{carb}$ was −12.7‰ between 0 and 20.07 m-levels, increased to −5.5‰ at 635 m-level of the core, and gradually decreased and stayed at around −13.0‰.

Fig. 4 shows the plots of the $\delta^{13}C_{carb}$ and $\delta^{18}O_{carb}$ values of the carbonate samples in this study, together with the data in literature. The $\delta^{13}C_{carb}$ and $\delta^{18}O_{carb}$ values varied between −2.0 and +4.5‰ and between −16.0 and −5.0‰, respectively, with the correlation coefficient of 0.18. On the basis of the $\delta^{13}C_{carb}$–$\delta^{18}O_{carb}$ diagram, the samples were statistically divided into the following three distinct distributions tentatively called Groups A, B, and C in this article. Group A includes the samples gathered around $\delta^{13}C_{carb} = -0.2$‰ and $\delta^{18}O_{carb} = -11.0$‰ at left side of lower part of all sample population and distinguished from the all Permian samples (Korte et al., 2005); Group B, the samples congregated around $\delta^{13}C_{carb} = +1.4$‰ and $\delta^{18}O_{carb} = -7.9$‰ in the lower part of all Permian samples (Korte et al., 2005); and Group C, the samples clustered far below the population of all Permian samples (Korte et al., 2005).

As for samples in Groups A and B, the $\delta^{13}C_{carb}$ values scattered around the least squared fitted line, $y = 1.3\ x - 11.0$, with the correlation coefficient of 0.78, indicating that the $\delta^{13}C_{carb}$ increased with increasing the $\delta^{18}O_{carb}$ value.

5. Discussion

5.1. Carbon isotopic composition of the least altered samples

In general, altered parts of carbonate sample are typically enriched in Mn and Fe, while depleted in $\delta^{13}C_{carb}$ and $\delta^{18}O_{carb}$ values with respect to unaltered parts (Brand and Veizer, 1981). By this matter, a $\delta^{13}C_{carb}$–$\delta^{18}O_{carb}$ diagram has been often used to check a degree of diagenetic alteration of carbonates. Fig. 4 shows all the previously reported $\delta^{13}C_{carb}$ and $\delta^{18}O_{carb}$ values of the Permian samples, including those of whole rocks and brachiopods of the Wordian (Korte et al., 2005), together with the samples in A, B, and C obtained in this work.

The $\delta^{13}C_{carb}$ and $\delta^{18}O_{carb}$ values of the Group B, which are statistically distinguishable from the Group A (Fig. 4), closely concentrated around their mean values in Fig. 4: $\delta^{13}C_{carb} = +2.7$‰ ($s = 1.0$‰) and $\delta^{18}O_{carb} = -7.2$‰ ($s = 1.1$‰). Notably, the samples in Group B are very close in the $\delta^{13}C_{carb}$ and $\delta^{18}O_{carb}$ values to the Wordian whole rock samples. As far as the $\delta^{13}C_{carb}$ is concerned, the samples in Group B are not distinct from the well-preserved Wordian brachiopods, although their $\delta^{18}O_{carb}$ is slightly lower than those of the brachiopod samples. From a view of the $\delta^{18}O$-axis, the samples in Group B occurs in the lower half of the main population of all of the Permian samples, and are almost identical to the Wordian whole rocks. Nonetheless, from a view of the $\delta^{13}C$-axis, the samples in Group B are nearly identical to the main population.

On the other hand, the samples in Group A are concentrated in an isotopically light region (low $\delta^{13}C_{carb}$ and low $\delta^{18}O_{carb}$) with respect to Group B, and are apparently different from the main population of all Permian samples. A similar negative trend in the $\delta^{13}C_{carb}$ and $\delta^{18}O_{carb}$ values was seen in the isotopic study of the Permian brachiopod shells; both isotopic values simultaneously became lighter with increasing a diagenetic artifact (Mii et al., 1997). Likewise, the similar trend was reported as a result of a late-stage burial diagenesis at elevated

Table 1
Analytical results on carbon and oxygen isotopic compositions of limestone samples from the Kaerimizu core no.1 section. The fusuline zones reported by Nakazawa and Ueno (2004) are shown. The samples with two index taxa, i.e. Verbeekina verbeeki and Colania douvillei were marked (X).The first occurrence position of C. douvillei in this core samples reported by Nakazawa and Ueno (2004) was confirmed in this study.

Sample name	Thickness of core (m)	Fusuline Zones	*Verbeekina verbeeki*	*Colania douvillei*	$\delta^{13}C_{carb}$ vs. PDB (‰)		$\Delta^{13}C_{carb}$ (Utrecht–Tsukuba)	$\delta^{18}0_{carb}$ vs. PDB (‰)		$\Delta^{18}0_{carb}$ (Utrecht–Tsukuba)
		Nakazawa and Ueno (2004)			Utrecht	Tsukuba		Utrecht	Tsukuba	
AK1-1	1.70	*N. simplex*								
AK1-2	3.45	*N. simplex*								
AK1-3	4.70	*N. simplex*				+3.2			-12.7	
AK1-4	6.90	*N. simplex*								
AK1-5	8.25	*N. simplex*								
8.80- 9.20 breccia										
AK1-6	9.50	*N. simplex*								
AK1-7	11.30	*N. simplex*								
AK1-8	15.75	*Parafusulina kaerimizuensis*								
AK1-9	17.50	*Parafusulina kaerimizuensis*								
AK1-10	19.10	*Parafusulina kaerimizuensis*								
AK1-11	20.07	*Parafusulina kaerimizuensis*				+4.1			-12.7	
AK1-12	21.90	*Parafusulina kaerimizuensis*								
AK1-13	25.67	*Parafusulina kaerimizuensis*								
AK1-14	26.25	*Parafusulina kaerimizuensis*								
26.60-26.90 vein										
AK1-15	27.30	*Parafusulina kaerimizuensis*				+4.2			-14.5	
AK1-16	29.08	*Parafusulina kaerimizuensis*				+4.0			-13.1	
AK1-17	30.70	*Parafusulina kaerimizuensis*				+4.2			-13.5	
AK1-18	31.33	*Parafusulina kaerimizuensis*				+4.2			-13.9	
AK1-19	33.05	*Parafusulina kaerimizuensis*				+4.2			-13.1	
AK1-20	33.94	*Parafusulina kaerimizuensis*				+3.7			-15.9	
AK1-21	35.55	*Afganella ozawaei*								
AK1-22	37.40	*Afganella ozawaei*				+4.2			-6.8	
AK1-22a	37.50	*Afganella ozawaei*				+3.9			-12.4	
AK1-23	38.68	*Afganella ozawaei*				+3.6			-15.8	
AK1-24	40.50	*N. craticufera robusta*								
AK1-25	40.60	*N. craticufera robusta*								
AK1-26	41.08	*N. craticufera robusta*				+3.9			-14.8	
AK1-27	42.90	*N. craticufera robusta*				+3.6			-8.3	
AK1-28	43.55	*N. craticufera robusta*				+2.1			-13.4	
AK1-29	44.98	*N. craticufera robusta*				+3.3			-8.0	
AK1-30a	46.68	*N. craticufera robusta*				+2.0			-13.5	
AK1-30	46.70	*N. craticufera robusta*				+3.1			-9.1	
AK1-301	47.45	*N. craticufera robusta*				+3.5			-15.1	
AK1-31	48.15	*N. craticufera robusta*				+1.3			-11.0	
AK1-311	48.62	*N. craticufera robusta*				+2.5			-7.1	
AK1-32	49.84	*N. craticufera robusta*				+0.1			-9.3	
50.40 disturbed (?)										
AK1-321	50.56	*N. craticufera robusta*				+2.1			-13.0	
		V. verbeeki–A. schencki								
56.70-57.10 vein										
AK1-33	58.27	*V. verbeeki–A. schencki*				+4.1			-7.1	
AK1-34	59.12	*V. verbeeki–A. schencki*				+4.0			-6.7	
AK1-35	60.28	*N. fusiformis*				+4.0			-5.5	
AK1-36	61.00	*N. fusiformis*				+3.5			-5.6	
AK1-37	61.43	*N. fusiformis*								
AK1-38	61.92	*N. fusiformis*								
AK1-39	63.50	*N. fusiformis*				+2.3			-5.5	
AK1-40	66.00	*N. fusiformis*				+2.2			-5.7	
AK1-41	68.76	*N. fusiformis*								
AK1-42	71.25	*V. verbeeki*				+1.5			-7.0	
AK1-43	71.34	*V. verbeeki*								
AK1-44	71.48	*V. verbeeki*								
AK1-45	72.25	*V. verbeeki*								
AK1-46	72.35	*V. verbeeki*								
AK1-47	72.95	*V. verbeeki*								
vain?										
AK1-48	73.00	*V. verbeeki*								
AK1-49	73.14	*V. verbeeki*								
AK1-50	73.25	*V. verbeeki*								
AK1-51	73.50	*V. verbeeki*				+1.2			-9.2	
AK1-52	74.17	*V. verbeeki*								
AK1-53	74.30	*V. verbeeki*								
AK1-54	74.41	*V. verbeeki*								

Table 1 (*continued*)

Sample name	Thickness of core (m)	Fusuline Zones	*Verbeekina verbeeki*	*Colania douvillei*	$\delta^{13}C_{carb}$ vs. PDB (‰)		$\Delta^{13}C_{carb}$ (Utrecht–Tsukuba)	$\delta^{18}O_{carb}$ vs. PDB (‰)		$\Delta^{18}O_{carb}$ (Utrecht–Tsukuba)
		Nakazawa and Ueno (2004)			Utrecht	Tsukuba		Utrecht	Tsukuba	
vain?										
AK1-55	74.53	*Colania douvillei*		×						
AK1-56	74.72	*Colania douvillei*								
AK1-57	75.49	*Colania douvillei*								
AK1-58	75.85	*Colania douvillei*			+1.8	+1.8	0.0	-7.5	-7.7	+0.1
AK1-59	76.62	*Colania douvillei*				+2.1			-7.8	
AK1-60	76.76	*Colania douvillei*				+2.1			-7.0	
AK1-61	77.30	*Colania douvillei*			+2.9	+2.9	0.0	-6.2	-6.4	+0.1
AK1-62	77.97	*Colania douvillei*				+1.4			-7.9	
AK1-63	78.20	*Colania douvillei*		×		+1.7			-8.6	
AK1-64	78.50	*Colania douvillei*				+1.8			-7.7	
AK1-65	79.50	*Colania douvillei*	×	×	+3.5	+3.5	0.0	-8.3	-8.5	+0.2
AK1-66	84.70	*Colania douvillei*			+0.3	+0.4	-0.1	-10.1	-10.2	+0.1
AK1-67	85.56	*Colania douvillei*			-1.5	-1.5	-0.1	-11.1	-11.3	+0.2
AK1-68	87.68	*Colania douvillei*	×	×	-0.1	-0.3	0.2	-12.9	-12.9	0.0
AK1-69	88.92	*Colania douvillei*	×		0.0	+0.1	-0.1	-11.0	-10.9	-0.2
AK1-70	89.92	*Colania douvillei*		×	0.0	+0.2	-0.2	-11.8	-11.5	-0.3
AK1-71	90.03	*Colania douvillei*	×	×	+0.6	+0.8	-0.2	-8.3	-8.1	-0.2
AK1-72	92.35	*Colania douvillei*		×	+0.4	+0.5	-0.1	-8.5	-8.4	-0.1
AK1-73	93.16	*Colania douvillei*	×		-0.4	-0.3	-0.2	-10.1	-9.9	-0.2
AK1-74	93.26	*Colania douvillei*	×		-1.4	-1.3	-0.1	-12.2	-11.8	-0.3
AK1-75	94.40	*Colania douvillei*		×	-0.1	-0.1		-13.1	-13.1	
AK1-76	94.90	*Colania douvillei*		×	0.0	-0.4		-13.2	-13.2	
AK1-77	95.40	*Colania douvillei*		×	-0.2	-0.2		-10.1	-10.1	
AK1-78	96.00	*Colania douvillei*		×	-0.5	-0.5		-10.6	-10.6	
AK1-79	97.10	*Colania douvillei*		×	0.0	0.0		-14.0	-14.0	
AK1-80	97.63	*Colania douvillei*		×	-0.4	-0.4		-14.2	-14.2	
AK1-81	98.10	*Colania douvillei*		×	-0.5	-0.5		-9.9	-9.9	
AK1-82	98.40	*Colania douvillei*		×	-0.5	-0.5		-11.4	-11.4	
AK1-83	98.67	*Colania douvillei*		×	-0.1	-0.1		-14.8	-14.8	
AK1-84	98.91	*Colania douvillei*		×	-0.6	-0.6		-14.7	-14.7	
AK1-85	99.46	*Colania douvillei*		×	+0.5	+0.5		-9.9	-9.9	
AK1-86	100.00	*Colania douvillei*		×	+0.2	+0.2		-11.4	-11.4	
AK1-87	104.00	*Colania douvillei*				-0.3			-12.7	
AK1-88	109.00	*Colania douvillei*				-1.0			-14.9	
AK1-89	111.00	*Colania douvillei*				-0.8			-15.0	
AK1-90	120.00	*Colania douvillei*				-2.1			-12.7	
AK1-91	136.00	*Colania douvillei*				-0.7			-12.7	
AK1-92	148.00	*Colania douvillei*				+0.3			-13.3	
AK1-93	154.00	*Colania douvillei*				-0.4			-12.1	
AK1-94	159.40	*Colania douvillei*				-0.3			-9.6	
AK1-95	159.90	*Colania douvillei*				-0.1			-10.7	
AK1-96	160.40	*Colania douvillei*				-0.2			-7.9	
AK1-97	160.90	*Colania douvillei*				-0.8			-11.2	
AK1-98	161.40	*Colania douvillei*				-0.7			-11.3	
AK1-99	161.70	*Colania douvillei*				-0.9			-10.1	
AK1-100	162.00	*Colania douvillei*				-0.6			-11.2	
AK1-101	162.06	*Colania douvillei*				-0.7			-12.5	
AK1-102	162.63	*Colania douvillei*				-0.9			-11.1	

temperature (i.e., Choquette and James, 1987). As for carbon isotopes, the primary carbonates isotopically equilibrated with ambient seawater may have become depleted during the diagenesis by influence of the isotopically light sources such as CO_2 dissolved in meteoric water and/or an oxidized organic matter in burial (Veizer, 1992).

The $\delta^{13}C_{carb}$ of the samples in Group C are within a range of those of all Permian samples, although their $\delta^{18}O_{carb}$ values are deviated far from those of the all Permian samples. The $\delta^{18}O_{carb}$ might severely affected by the meteoric water alteration, whereas the $\delta^{13}C_{carb}$ may be less suffer from the diagenesis with the meteoric water and/or the oxidized organic matter.

Excluding the samples in Group C, all of the samples in Fig. 4 seem to be proportional between the $\delta^{13}C_{carb}$ and $\delta^{18}O_{carb}$ values: the $\delta^{13}C_{carb}$ increases with increasing $\delta^{18}O_{carb}$ value. This tendency may indicate a degree of alteration of the original carbonates by meteoric water. For instance, carbonate rocks undergone a diagenetic stage can all potentially make the $\delta^{18}O$ values lower (Jaffrés et al., 2007). Moreover, Mii et al. (1997) pointed out that the primary $\delta^{18}O_{carb}$ values of the carbonate samples could decrease more than 9.0‰ by diagenetic artifacts. Such samples typically show very light isotopic compositions, which are less than −10.0‰ in $\delta^{18}O_{carb}$. Assuming that the samples in Group B are better preserved isotopically rather than those in Group A, only if the meteoric water alteration of the carbonates solely caused the synchronous reduction of the $\delta^{13}C_{carb}$ and $\delta^{18}O_{carb}$ values, $\delta^{13}C_{carb} = +2.7‰$ ($s = 1.0‰$) and $\delta^{18}O_{carb} = -7.2‰$ ($s = 1.1‰$) could be the average isotopic values of the least altered Akiyoshi carbonates. Comparing the data to specific examples from the published literatures, whole rock samples from the Wordian and Capitanian show a varied range of $\delta^{13}C = +2$ to $+4‰$ with $\delta^{18}O = -5$ to $-10‰$ (Korte et al., 2005) that is nearly equal to those of Group B. In addition, non-luminescent and slightly luminescent part of the Permian brachiopods with silicification (Appendix I in Mii et al., 1997) had similar range in $\delta^{13}C$ and $\delta^{18}O$ to Group B.

As a summary, judging from the $\delta^{13}C_{carb}$–$\delta^{18}O_{carb}$ diagram (Fig. 4), the $\delta^{13}C_{carb}$ values of the samples in Groups B and C are less altered among the Kaerimizu core samples. They likely preserved the primary $\delta^{13}C$ record of the Permian seawater signals, only if diagenesis was less effective.

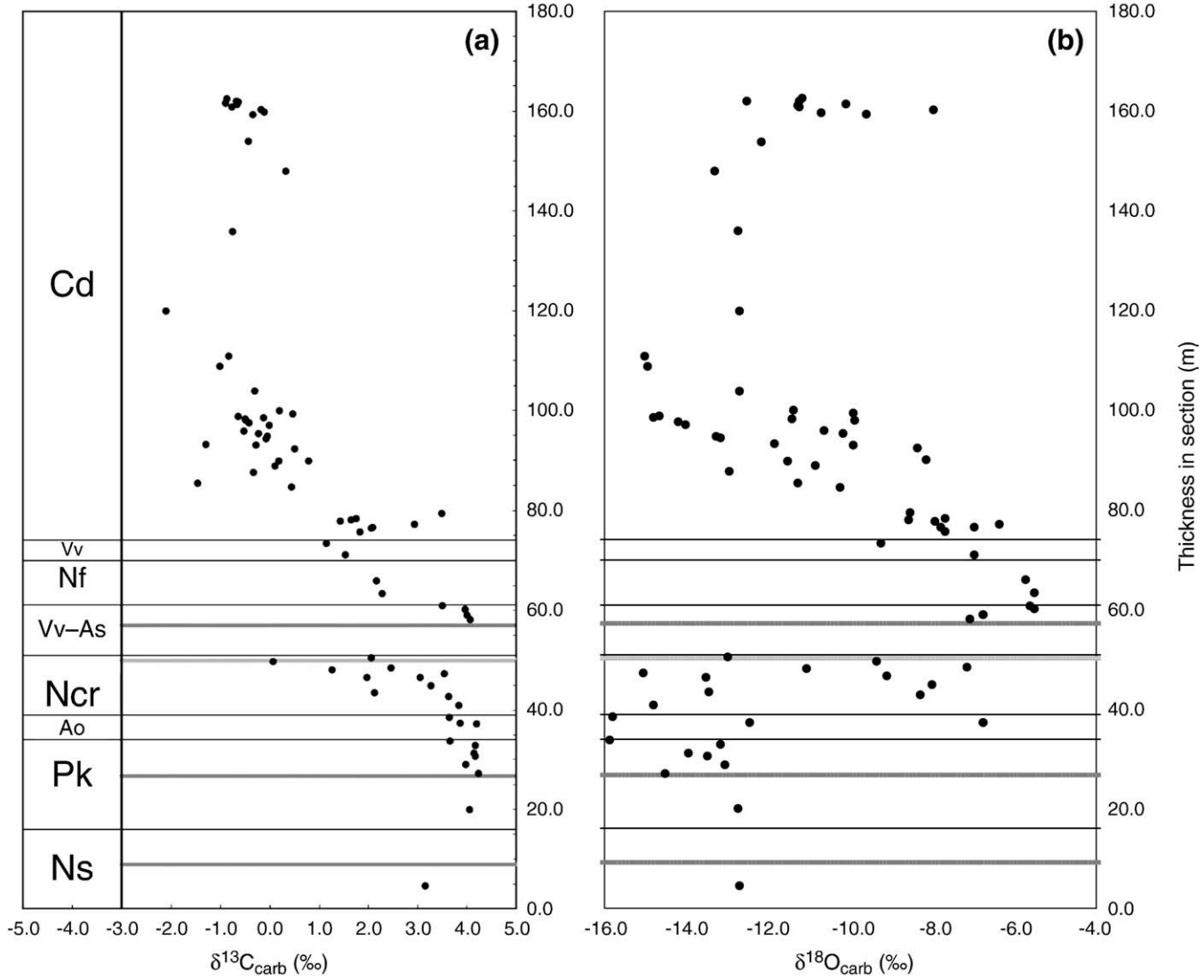

Fig. 3. Secular changes in the (a) $\delta^{13}C_{carb}$ and (b) $\delta^{18}O_{carb}$ values of the limestone samples from the Kaerimizu no. 1 drilled core. Horizontal dotted lines indicate potential stratigraphic breaks indicated by breccias and concentrated veins.

5.2. Secular change of the selected $\delta^{13}C$ values during the Early–Middle Guadalupian

On the basis solely on the $\delta^{13}C_{carb}$ values of Groups B and C, Fig. 5a shows the secular change of the $\delta^{13}C_{carb}$ values along the stratigraphic column of the studied section. The 21 samples of Group B and 15 samples of Group C are plotted here as (●) and (Δ), respectively (Fig. 5a).

The $\delta^{13}C_{carb}$ values are mostly stable around +4.0‰ during the *Pk* Z., and gradually decrease from the top of the *Pk* Z. through the *Ao* Z. to the *Cd* Z. (Fig. 5). Going into the details, the $\delta^{13}C_{carb}$ values of samples in Group B (●) fluctuate between +1.0 and +4.0‰ during the interval between the *Ao* and *Cd* zones. On the other hand, those of samples in Group C (Δ) are mostly concentrated around +4.0‰ in the *Pk* and *Ncr* zones, except three samples in the *Ncr* Z. (+2.0‰). Notably, the $\delta^{13}C_{carb}$ values of Group C in the *Ncr* Z. apparently shift negatively with the gradual ^{13}C-depletion of the samples in Group B. Similarly, in the interval of the *Vv–As*, *Nf*, *Vv*, and *Cd* zones (between 60 and 80 m-levels), the $\delta^{13}C_{carb}$ values (●) again negatively shift from +4.0‰ to +1.0‰.

The reason of these negative shifts is still unknown; however, the brecciation found at 50.4 m at the top of the *Ncr* Z (Figs. 2 and 3) and the concentrated development of calcite veins at 57 m and 72 m-levels suggest a stratigraphic disturbance that may have been responsible for the acute ^{13}C-depletion depletion (Fig. 5). In general, diagenetic alteration commonly reduces a $\delta^{13}C_{carb}$ value if an isotopically light source, such as the meteoric water with dissolved CO_2, penetrates and influences carbonate sediments (Veizer, 1992), particularly along disturbed zone. As a rest of the section is likely free from such a post-sedimentary disturbance, we evaluate the higher value (+4.0‰) as a better preserved primary signature.

Recently $\delta^{13}C_{carb}$ values in the Wordian interval were reported from the lower part of the Iwato Formation in Kyushu, SW Japan (Isozaki et al., 2007b), that is biostratigraphically correlated in part with the Kaerimizu section (Ota and Isozaki, 2006). The $\delta^{13}C_{carb}$ values are relatively high positive between +4.0 and +6.0‰, and demonstrate an upward increase trend from +3.5‰ to +4.3‰ that begins in the *Neoschwagerina* Zone (Fig. 5b) (Isozaki et al., 2007a,b). Although $\delta^{13}C_{carb}$ values fluctuate in the upper Wordian interval, the lower half of the Kaerimizu section is by and large correlated chemostratigraphically with the lower Iwato Formation.

It is noteworthy that the Iwato Formation was derived from a different chain of seamounts located in a distinct part of the superocean Panthalassa during the Permian, and was accreted to

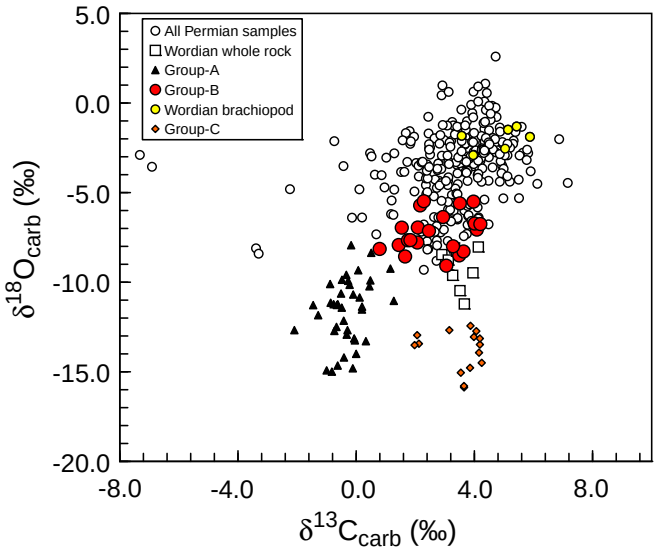

Fig. 4. Correlation between $\delta^{13}C_{carb}$ and $\delta^{18}O_{carb}$ values of the Permian carbonate samples. The open circles indicate the values of the Permian carbonate samples cited from Korte et al. (2005). The open squares and the circles filled in dark gray color represent samples of theWordian whole rocks and those of theWordian brachiopods, respectively (Korte et al., 2005). The bold triangles, the bold circles, and the lightly gray diamonds are the Akiyoshi limestone samples belonging to Group A, B, and C, respectively.

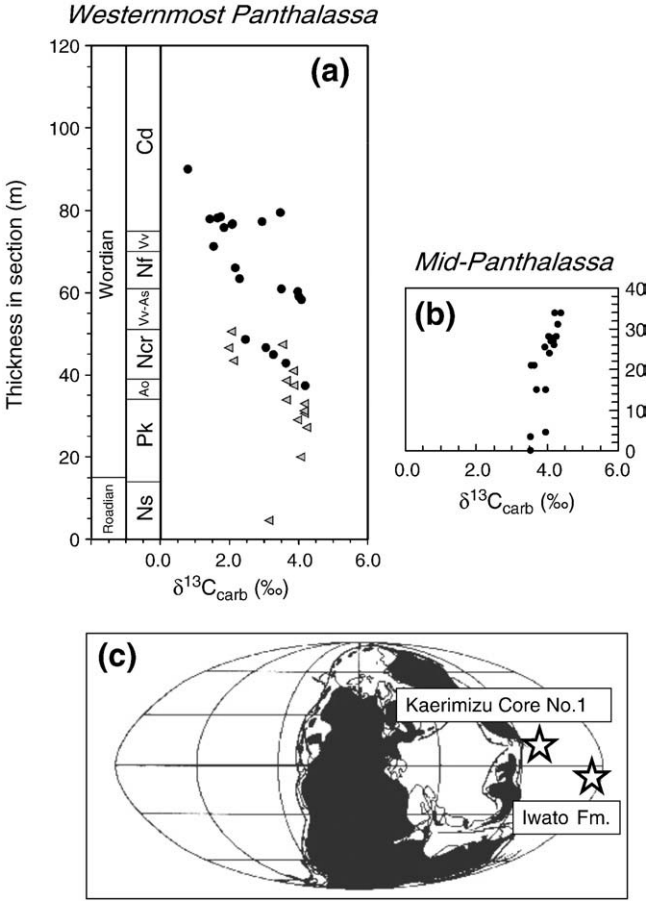

Fig. 5. Secular changes of the $\delta^{13}C_{carb}$ values of (a) the selected samples in Kaerimizu no.1 section (*westernmost Panthalassa*), and (b) the samples of the Iwato Formation (*mid-Panthalassa*) reported by Isozaki et al. (2007a,b). For (a), the samples in Group B were indicated by the bold circles for $\delta^{13}C_{carb}$ and those in Group C were represented by the triangles for $\delta^{13}C_{carb}$. The fusuline zones (Nakazawa and Ueno, 2004) are abbreviated as follows; Ns: *Neoschwagerina simplex* Zone; Pk: *Parafusulina kaerimizenis* Zone; Ao: *Afghanella ozawai* Zone; Ncr: *Neoshwagerina craticulifera robusta* Zone; Vv-As: *Verbeekina verbbbki-Afghanella schencki* Zone; Nf: *Neoschwagerina fusiformis* Zone; Vv: *Verbbkina verbeeki* Zone; and Cd: *Colania douvillei* Zone. For (b), the vertical axis indicates the thickness in core. The interval of the (b) is approximately correlated to that between 21 and 61 m of the (a), since the *N. craticulifera robusta* was first occurred in 21 m of the (b). (c) The location of the Akiyoshi and Iwato (Kamura) paleo-seamounts in Late Permian.

Japan margin in the Middle Jurassic, i.e., nearly 100 million years later than the accretion of the Akiyoshi Limestone (Isozaki, 1997a; Ota and Isozaki, 2006). New paleomagnetic data indicate that the Iwato Formation was deposited at 12° S (Kirschvink and Isozaki, 2007). Given the average rate of plate convergence around 3 cm/year, this time lag of nearly 100 million years corresponds up to 3000 km in geographical separation between the seamount and subduction zone. Thus the Iwato paleo-seamount was located somewhere in the equatorial mid-Panthalassa in the southern hemisphere (Fig. 5c). In contrast, the Akiyoshi paleo-seamount was located almost next to a trench along Japan (South China) margin probably in low-latitude in the northern hemisphere immediately before the final accretion (Isozaki, 1997a). Thus the intimate bio- and chemostratigraphic correlation between the Akiyoshi limostone and the Iwato Formation strongly suggests that the central and westernmost Panthalassa was extensively occupied by a water mass with heavy C isotope signature.

5.3. Middle Guadalupian onset of high productivity

The better preserved samples selected on the basis of the $\delta^{13}C_{carb}$–$\delta^{18}O_{carb}$ diagram (Fig. 4) show that a high positive $\delta^{13}C_{carb}$ interval in the Wordian. The high positive interval occurred ubiquitously in the Wordian shallow marine carbonates not only in the Akiyoshi Limestone but also in the Iwato Formation in Japan (Fig. 5a,b). The positive $\delta^{13}C_{carb}$ values suggest that carbonate dissolved in surface seawater may have thoroughly enriched in isotopically heavier carbon (^{13}C) at least in the central to westernmost low-latitude Panthalassa. High $\delta^{13}C_{carb}$ values up to +7.5‰ were also reported from the coeval carbonates in Svalbard (Mii et al., 1997), west Texas, the Sverdrup Basin (Canada), and northern Spain (Grossman et al., 2008). These suggest that the high $\delta^{13}C_{carb}$ values during this time interval was a global signature for the Wordian.

The ^{13}C-enrichment was likely caused by the increased burial of organic carbon that preferentially removed ^{12}C from seawater. If this is the case, the high $\delta^{13}C_{carb}$ values suggest that photosynthesis-driven primary productivity has become high already in the Wardian, at least around the Akiyoshi and Iwato paleo-seamount in the superocean Panthalassa. The other possible cause of the ^{13}C-enrichment was an addition of the formatized organic carbon (up to +15‰) to coeval carbonates during diagenetic process, if any, as it was the case in a study on the ^{13}C-enriched dolomites from Guaymas Basin. The latter explanation is, however, unlikely for the less dolomitized Akiyoshi Limestone.

The period of high positive plateau of the $\delta^{13}C_{carb}$ values over +5.0‰ in the upper part of the Iwato Formation (Capitanian) likely represents a cooling period (or the Kamura cooling event by Isozaki et al., 2007a,b). This putative cooling might have affected also the westernmost part of Panthalassa. Isozaki (2009a,b) explained that the Kamura cooling may have been caused by a major change in geodynamo of the Earth's outer core in association with the launching of a superplume.

In short, the present study confirmed that the surface water of Panthalassa had $\delta^{13}C_{carb}$ values of ca. +3.5‰ to +4.0‰ during the Wordian, immediately before the Capitanian Kamura event. This result constrains that the onset of the Kamura cooling event was likely in the Early Capitanian, and the Wordian interval with high $\delta^{13}C_{carb}$ values may represent a prelude of the Kamura event. Our results suggest positive links to the recent findings of the rapid change in atmospheric pCO_2 and to the coeval glacial deposits in Gondwana during the Guadalupian (Fielding et al., 2008).

6. Conclusions

We investigated the isotopic compositions of the inorganic carbon and the oxygen ($\delta^{13}C_{carb}$ and $\delta^{18}O_{carb}$ vs. PDB) of the Guadalupian (Middle Permian) shallow marine carbonates of the Akiyoshi Limestone in Southwest Japan that primarily deposited on an ancient seamount in the low-latitude Panthalassa. By extracting statistically $\delta^{13}C_{carb}$ and $\delta^{18}O_{carb}$ values from alteration-free samples, we obtain relatively high $\delta^{13}C$ values for the Wordian interval. This indicates that the primary productivity was relatively high already in the Wordian in the westernmost Panthalassa but not yet reached to the maximum level before the start of the Kamura event in the Capitanian.

Acknowledgements

We thank Takehiko Haikawa, the chief curator of Akiyoshi-dai Museum of Natural History, for providing us the samples from Kaerimizu. We also acknowledge Hisayoshi Igo of Institute of Natural History for identification of fusulines and Kayo Minoshima of Geological Survey of Japan, AIST, for her assistance of the isotope analysis. This research was partly supported by the Grant-in Aid of Japan Society of Promoting Science (no. 20224012).

References

Baud, A., Magaritz, M., Holser, W.T., 1989. Permian–Triassic of the Tethys — carbon isotope studies. Geologische Rundschau 78, 649–677.

Brand, U., Veizer, J., 1981. Chemical diagenesis of a multicomponent carbonate system -2: stable isotopes. Journal of Sedimentary Petrology 51, 987–997.

Choquette, P.W., James, N.P., 1987. Diagenesis in limestones, 3. The deep burial environment. Geoscience Canada 14, 3–35.

Fielding, C.R., Frank, T.D., Birgenheier, L.P., Rygel, M.C., Jones, A.T., Roberts, J., 2008. Stratigraphic imprint of the Late Palaeozoic Ice Age in eastern Australia: a record of alternating glacial and nonglacial climate regime. Journal of the Geological Society 165, 129–140.

Grossman, E.L., Yancey, T.E., Jones, T.E., Bruckschen, P., Chuvashov, B., Mazzullo, S.J., Mii, H.-S., 2008. Glaciation, aridification, and carbon sequestration in the permo-carboniferous: the isotopic record from low latitudes. Palaeogeography, Palaeoclimatology, Palaeoecology. doi:10.1016/j.palaeo.2008.03.053.

Heydari, E., Hassanzadeh, J., Wade, W.J., Ghazi, A.M., 2003. Permian–Triassic boundary interval in the Abadeh section of Iran with implications for mass extinction: part 1—sedimentology. Palaeogeography Palaeoclimatology Palaeoecology 193, 405–423.

Isozaki, Y., 1997a. Permian–Triassic boundary superanoxia and stratified superocean: records from lost deep-sea. Science 276, 235–238.

Isozaki, Y., 1997b. Contrasting two types of orogen in Permo-Triassic Japan: accretionary versus collisional. The Island Arc 6, 2–24.

Isozaki, Y., 2009a. Illawarra Reversal: the fingerprint of a superplume that triggered Pangean breakup and the end-Guadalupian (Permian) mass extinction. Gondwana Research 15, 421–432.

Isozaki, Y., 2009b. Integrated plume winter scenario for the double-phased extinction during the Paleozoic–Mesozoic transition: the G–LB and P–TB events from a Panthalassan perspective. Journal of Asian Earth Sciences 36, 457–480.

Isozaki, Y., Ota, A., 2001. Middle–Upper Permian (Maokouan–Wuchiapingian) boundary in mid-oceanic paleo-atoll limestone of Kamura and Akasaka, Japan. Proceedings of Japan Academy 77B, 104–109.

Isozaki, Y., Kawahata, H., Ota, A., 2007b. A unique carbon isotope record across the Guadalupian–Lopingian (Middle–Upper Permian) boundary in mid-oceanic paleo-atoll carbonates: the high-productivity "Kamura vent" and its collapse in Panthalassa. Global Planetary Change 55, 21–38.

Isozaki, Y., Kawahata, H., Minoshima, K., 2007a. The Capitanian (Permian) Kamura cooling event: the beginning of the Paleozoic–Mesozoic transition. Palaeoworld 16, 16–30.

Jaffrés, J.B.D., Shields, G.A., Wallmann, K., 2007a. The oxygen isotope evolution of seawater: a critical review of a long-standing controversy and an improved geological water cycle model for the past 3.4 billion years. Earth-Science Review 83, 83–122.

Jin, Y.G., Zhang, J., Shang, Q.H., 1994. Two phases of the end-Permian mass extinction. In Embry, A.F., Beauchamp, B., Glass, D.J. (Eds.), Pangea: Global Environments and Resources. Memoir, Canadian Society of Petroleum Geologists 17, 813-822.

Kanmera, K., Nishi, H., 1983. Accreted oceanic reef complex in southwest Japan. In: Hashimoto, M., Ueda, S. (Eds.), Accretion tectonics in the circum-Pacific regions: Terra Science, Tokyo, pp. 195–206.

Kanmera, K., Sano, H., Isozaki, Y., 1990. Akiyoshi terrane. In: Ichikawa, K., Mizutani, S., Hara, I., Hada, S., Yao, A. (Eds.), Pre-Cretaceous terranes of Japan. Publication IGCP-224, Osaka, pp. 49–62.

Kirschvink, J.L., Isozaki, Y., 2007. Extending the sensitivity of paleomagnetic techniques: magnetostratigraphy of weakly-magnetized, organic-rich black limestone from the Permian of Japan. EOS Transactions, American Geophysical Union 2007 AGU Fall Meeting, 88, 52(1), F881-F881, American Geophysical Union.

Korte, C., Jasper, T., Kozur, H.W., Veizer, J., 2005. $\delta^{18}O$ and $\delta^{13}C$ of Permian brachiopods: a record of seawater evolution and continental glaciation. Palaeogeography, Palaeoclimatology, Palaeoecology 224, 333–351.

Maruyama, S., Isozaki, Y., Kimura, G., Terabayashi, M., 1997. Paleogeographic maps of the Japanese Islands: plate tectonic synthesis from 750 Ma to the present. The Island Arc 6, 121–142.

Mii, H.-S., Grossman, E., Yancey, T.E., 1997. Stable carbon and oxygen isotope shifts in Permian seas of West Spitsbergen — global change or diagenetic artifact? Geology 58, 227–230.

Musashi, M., Isozaki, Y., Koike, T., Kreulen, R., 2001. Stable carbon isotope signature in mid-Panthalassa shallow-water carbonates across the Permo-Triassic boundary: evidence for ^{13}C-deleted ocean. Earth and Planetary Science Letters 191, 9–20.

Musashi, M., Isozaki, Y., Koike, T., Kreulen, R., 2007. Carbon isotope study on mid-Panthalassa shallow-water limestone across the Permo-Triassic boundary. In: Wong, T. (Ed.), Reassessment: The Royal Netherlands Academy of the Art and Sciences Special Publication, pp. 131–138.

Nakazawa, T., Ueno, K., 2004. Sequence boundary and related sedimentary and diagenetic facies formed on Middle Permian mid-oceanic carbonate platform: core observation of Akiyoshi Limestone, Southwest Japan. Facies 50, 301–311.

Ota, M., 1977. Geological studies of Akiyoshi: part 1. General geology of the Akiyoshi Limestone Group: Bulletin of Akiyoshi-dai Museum of Natural History, vol. 12, pp. 1–33.

Ota, A., Isozaki, Y., 2006. Fusuline biotic turnover across the Guadalupian–Lopingian (Middle–Upper Permian) boundary in mid-oceanic carbonate buildups: biostratigraphy of accreted limestone in Japan. Journal of Asian Earth Sciences 26, 353–368.

Ota, M., Toriyama, R., Sugimura, A., Haikawa, T., 1973. Restudy on the geologic structure of the Akiyoshi Limestone Group. Southwest Japan. Chigaku-zasshi 82, 1–21 (in Japanese with English abstract).

Sano, H., 2006. Impact of long-term climate change and sea-level fluctuation on Mississippian to Permian mid-oceanic atoll sedimentation (Akiyoshi Limestone Group, Japan). Palaeogeography, Palaeoclimatology, Palaeoecology 236, 169–189.

Sano, H., Kanmera, K., 1988. Paleogeographic reconstruction of accreted oceanic rocks, Akiyoshi, southwest Japan. Geology 16, 600–603.

Stanly, S.M., Yang, X., 1994. A double mass extinction at the end of the Paleozoic era. Science 266, 1340–1344.

Suzuki, A., Kawahata, H., Tanimoto, Y., Tsukamoto, H., Gupta, L.P., Yukino, I., 2000. Skeletal isotopic record of a Porites coral during the 1998 mass bleaching event. Geochemical Journal 34, 321–329.

Ueno, K., 1992. Verbeekinid and neoschwagerinid fusulinaceans from the Akiyoshi Limestone Group above the Parfusulina kaerimizensis zone, southwest Japan. Transaction Proceedings of Paleontological Society of Japan, N.S. 165, 1040–1069.

Ueno, K., 1996. Verbeekinid and neoschwagerinid fusulinaceans from the Akiyoshi Limestone Group above the Parafusulina kaerimizensis zone, southwest Japan. Transaction Proceedings of Paleontological Society of Japan, N.S. 165, 1040–1069.

Veizer, J., 1992. Depositional and diagenetic history of limestones: stable and radiogenic isotopes. Isotopic signatures and sedimentary records: Lecture notes in earth sciences, vol. 43, pp. 13–48.

Wang, W., Cao, C.Q., Wang, Y., 2004. The carbon isotope excursion on GSSP candidate section of Lupiangian–Guadalupian boundary. Earth and Planetary Science Letters 220, 57–67.